

## Quasipatterns in a Model for Chemical Oscillations Forced at Multiple Resonance Frequencies

Jessica M. Conway and Hermann Riecke

*Engineering Sciences and Applied Mathematics, Northwestern University, Evanston, Illinois 60208, USA*  
(Received 28 March 2007; published 21 November 2007)

Multifrequency forcing of systems undergoing a Hopf bifurcation to spatially homogeneous oscillations is investigated. For weak forcing composed of frequencies near the 1:1, 1:2, and 1:3 resonances, such systems can be described systematically by a suitably extended complex Ginzburg-Landau equation. Weakly nonlinear analysis shows that, generically, the forcing function can be tuned such that resonant triad interactions with weakly damped modes stabilize subharmonic 4- and 5-mode quasipatterns. In simulations starting from random initial conditions, domains of these quasipatterns compete and yield complex, slowly ordering patterns.

DOI: [10.1103/PhysRevLett.99.218301](https://doi.org/10.1103/PhysRevLett.99.218301)

PACS numbers: 82.40.Ck, 42.65.Yj, 47.54.-r, 52.35.Mw

In recent years, complex but ordered spatiotemporal patterns characterized by multiple length scales have found considerable interest. In particular, on the surface of vertically vibrated fluid layers (Faraday system) various kinds of fascinating periodic superlattice patterns and quasipatterns have been found experimentally [1,2]. Subsequently, such patterns have also been observed in optical systems [3], in vertically vibrated fluid convection [4], and on the surface of ferrofluids driven by time-periodic magnetic fields [5]. Here we show that superlattices and quasipatterns should be accessible quite generally in a different class of systems: resonantly forced systems undergoing a Hopf bifurcation to spatially homogeneous oscillations. Paradigmatic for such systems are chemical oscillations [6]. In chemical systems, patterns with multiple length scales have so far been obtained only by imposing an external length through *spatially* periodic illumination [7].

The stability of multimode patterns depends on the interaction between their constitutive Fourier modes. For small angles  $\theta$  between the modes, the cross-coupling coefficient  $b(\theta)$  is twice as large as the self-coupling coefficient  $b_0$ . Nearly parallel modes therefore suppress each other, and, unless the cross-coupling coefficient decreases substantially with increasing  $\theta$ , only stripelike patterns are stable. Strong angle dependence can arise if the basic modes couple to weakly damped, resonating modes [8,9]. Complex patterns with different symmetries can then become stable [10].

The resonances stabilizing complex patterns have been studied in great detail in the Faraday system. Their spatio-temporal nature [11] allows a very controlled tuning through the frequency content of the driving [12]. Broadly speaking, there are two mechanisms by which complex patterns can be stabilized: either by enhancing damping via the self-coupling  $b_0$  [9,13,14] or by reducing the cross-coupling coefficient  $b(\theta)$  [12,14].

In this Letter, we exploit spatiotemporal resonances to induce complex spatial patterns in two-dimensional systems undergoing a Hopf bifurcation to spatially homo-

geneous oscillations. To this end, we apply spatially homogeneous, resonant multifrequency forcing. By including a frequency component close to twice the Hopf frequency  $\omega_h$  (1:2 resonance), we excite standing waves with a wave number determined by the detuning between the forcing and the Hopf frequency [15]. A second frequency near 3 times the Hopf frequency (1:3 resonance) induces a quadratic interaction term, which otherwise is not allowed in the normal form for Hopf bifurcations. To avoid transcritical bifurcations off the basic state to hexagonal patterns [16], we further include a second forcing frequency close to the 1:2 resonance with a slightly different detuning. Within the weakly nonlinear regime, we show that, quite independent of the two parameters characterizing the unforced Hopf bifurcation, the forcing function can be tuned such that instead of the usual stripe, spiral, and labyrinthine patterns [17] one obtains superlattices and quasipatterns.

The systematic, weakly nonlinear description of a weakly forced supercritical Hopf bifurcation is given by the complex Ginzburg-Landau equation for the complex oscillation amplitude  $A$ , which is extended to include the near-resonant components of the forcing function [18]:

$$\frac{\partial A}{\partial t} = (1 + i\beta)\nabla^2 A + [\mu + i\sigma - (1 + i\alpha)|A|^2]A + \gamma(\cos\chi + \sin\chi e^{i\nu t})A^* + \rho e^{i\Phi}A^{*2}. \quad (1)$$

Here  $\chi$  measures the relative contributions from the two forcing components that are close to the 1:2 resonance, which differ in their frequencies by  $\nu$ . The detuning between the Hopf frequency and half the frequency corresponding to the forcing  $\gamma \cos\chi$  is given by  $\sigma$ . The strength and phase of the 1:3 forcing are given by  $\rho$  and  $\Phi$ , respectively. Nonlinear interactions of the 1:2-resonant forcing and the 1:3-resonant forcing introduce an additional forcing near the Hopf frequency itself. For simplicity, we assume a further explicit forcing component near the 1:1 resonance that cancels the resulting additional, inhomogeneous term in (1). It is straightforward to derive

(1) from Oregonator-type models for the photosensitive Belousov-Zhabotinsky reaction [19].

The slight detuning between the two 1:2-forcing components introduces the explicit, periodic time dependence of the coefficients in (1). By using Floquet theory, we determine the instability of the basic state  $A = 0$  with respect to time-periodic solutions that are phase-locked to the forcing [19]. Because of the dispersion  $\beta$ , the detuning  $\sigma$  induces phase-locked modes with a nonzero wave number [15]. Depending on the forcing parameter  $\chi$  and the detuning  $\nu$ , the mode that destabilizes the basic state first is either harmonic or subharmonic relative to the period  $2\pi/\nu$ .

A typical set of neutral curves  $\gamma^{(H,SH)}(k)$  for the harmonic and subharmonic modes is shown in Fig. 1. We focus here on the subharmonic case. The competition between subharmonic modes of different orientation [11,13] is modified by weakly damped harmonic modes excited at quadratic order. Their effect is strongest if the forcing  $\gamma$  is only slightly below the critical forcing strength  $\gamma_c^{(H)}$  of the harmonic modes (inset in Fig. 1). For this reason, we tune the forcing parameter  $\chi$  and the detuning  $\nu$  so that  $\gamma_c^{(H)}$  is only slightly above the critical forcing strength  $\gamma_c^{(SH)}$  of the subharmonic modes. In this Letter, we focus on the enhancement of the self-coupling  $b_0$  of the subharmonic modes and choose the forcing function such that the critical wave number  $k_c^{(H)}$  of the harmonic mode is close to twice that of the subharmonic mode  $K \equiv k_c^{(H)}/k_c^{(SH)} \simeq 2$ . To reduce the competition between modes subtending a specific angle  $\theta$ , a wave-number ratio  $K < 2$  would be chosen [19].

To compute the interaction between modes of different orientation within weakly nonlinear analysis, we expand the oscillation amplitude as ( $\epsilon \ll 1$ )

$$A = \epsilon(A_1 e^{ik_1 \cdot r} + A_2 e^{ik_2 \cdot r})F(t) + \text{h.o.t.} \quad (2)$$

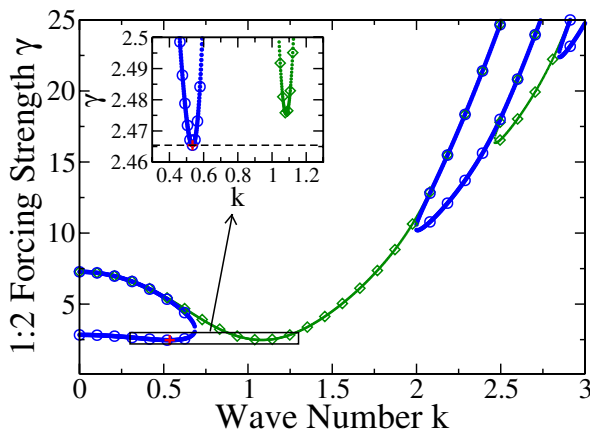


FIG. 1 (color online). Neutral curves for subharmonic (thick lines) and harmonic modes (thin lines) for  $\mu = -1$ ,  $\sigma = 4$ ,  $\beta = 3$ ,  $\chi = 0.476718$ , and  $\nu = 4.2$ .

For subharmonic patterns,  $F(t)$  has periodicity  $4\pi/\nu$ . Because of the time shift symmetry  $t \rightarrow t + 2\pi/\nu$ , the amplitude equations for  $A_{1,2}$  must be equivariant under the transformation  $A_{1,2} \rightarrow -A_{1,2}$ :

$$\frac{dA_1}{dt} = \lambda A_1 - b_0 A_1 |A_1|^2 - b(\theta) A_1 |A_2|^2, \quad (3)$$

with a similar equation for  $A_2$ . This symmetry eliminates all quadratic terms and the associated transcritical bifurcation.

Relevant for the pattern selection is the ratio  $b(\theta)/b_0$ . It is strongly affected by spatiotemporally resonant triads, which are induced by the 1:3 forcing  $\rho e^{i\Phi}$ . The resulting  $\rho$  dependence of  $b(\theta)/b_0$  is shown in Fig. 2. The stability conditions for rectangular patterns (corresponding to a rhombic arrangement of the wave vectors) are  $b_0 > 0$  and  $|b(\theta)/b_0| < 1$ . Thus, with increasing 1:3 forcing  $\rho$ , a large range of angles arises for which rectangular patterns are stable, whereas without that forcing only stripe patterns would be obtained. This is in contrast to the case of Faraday waves, where even single-frequency forcing often yields square patterns [2].

Given  $b(\theta)$ , the linear stability of various types of periodic superlattice patterns comprised of three or more modes on a fixed periodic Fourier lattice can be determined systematically [20]. For simplicity, we consider only patterns with Fourier modes that are equally spaced on the critical circle. They may not form a periodic Fourier lattice. This approach ignores possible higher-order resonances [21] and sideband instabilities [22] and does not account for possible convergence problems due to small divisors [23]. In Fig. 3, we show the relative stability of planforms contained in the subspaces spanned by 4, 5, and 6 equally spaced modes, respectively.

To address the competition between different, simultaneously stable planforms, we exploit the variational character of (3):  $\partial A_j / \partial T = -\partial F_N / \partial A_j^*$  for  $j = 1, \dots, N$ . Figure 3 shows the energies  $F_N$  of patterns comprised of

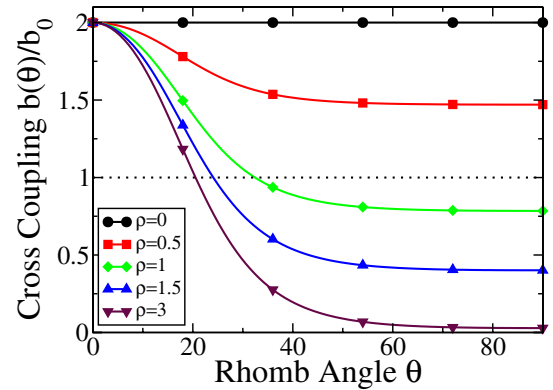


FIG. 2 (color online). Angle dependence of the effective cross coupling  $b(\theta)/b_0$  for  $\alpha = -1$  and  $\Phi = \frac{3\pi}{4}$ . Other parameters as in Fig. 1.

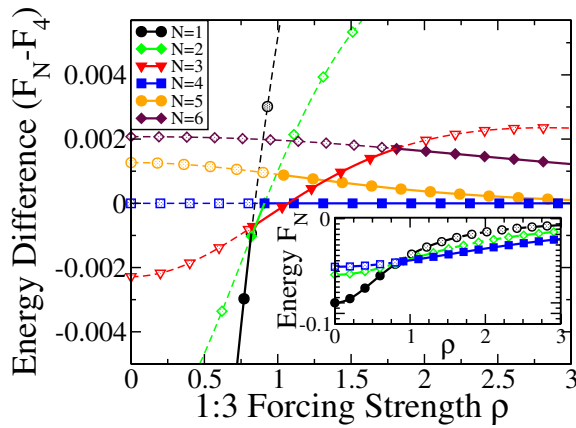


FIG. 3 (color online). Energy of planforms comprised of  $N$  Fourier modes. Parameters as in Fig. 2. Solid (open) symbols: Linearly stable (unstable) planforms.

$N$  modes that are equally spaced on the critical circle as a function of the 1:3-forcing strength  $\rho$ . When starting from random initial conditions, planforms with lower energy are expected to invade those with higher energy. Thus, for  $\rho \leq 0.82$ , the final state is expected to consist of stripes, whereas for  $\rho \geq 1.07$  patterns with four or more modes should dominate.

To test the predictions of our weakly nonlinear analysis, we perform direct simulations of the complex Ginzburg-Landau equation (1). For a small system size, they confirm the linear stability of patterns comprised of four modes. To investigate the dependence of the pattern selection on the 1:3-forcing strength  $\rho$ , we perform simulations in a large square system of linear size  $L = 2\pi/k_c^{(\text{SH})} \approx 473.39$  for increasing forcing strengths  $\rho$ , starting from *identical* random initial conditions. We choose the system size such that the modes making up hexagons and supersquares have equal linear growth rates to bring out clearly how an increase in  $\rho$  alone tips the balance from hexagons to fourfold patterns. For  $\rho = 0.9$ , a pattern with a hexagonal planform rather than a stripe structure arises. Because of the reflection symmetry  $A_j \rightarrow -A_j$  of (3), domains with up and down hexagons coexist separated by walls containing narrow layers of triangle patterns [19].

Increasing  $\rho$  decreases the  $\theta$  range over which modes suppress each other (cf. Figure 2) and more modes persist, as shown in Fig. 4 for  $\rho = 1.2$ . The pattern exhibits elements reminiscent of “supersquares” and “antisquares” [20] (marked by dashed-dotted and dashed circles, respectively). Increasing the 1:3 forcing to  $\rho = 2$  increases the number of persisting modes further and introduces numerous elements with fivefold and with tenfold rotational symmetry (dashed and solid circles, respectively) in Fig. 5.

The patterns shown in Figs. 4 and 5 are still evolving, albeit very slowly. Nevertheless, it is clear that for  $\rho \geq 1.1$  they will not evolve to simple hexagon states. While in our simulations for all values of  $\rho$  domains of hexagons ap-

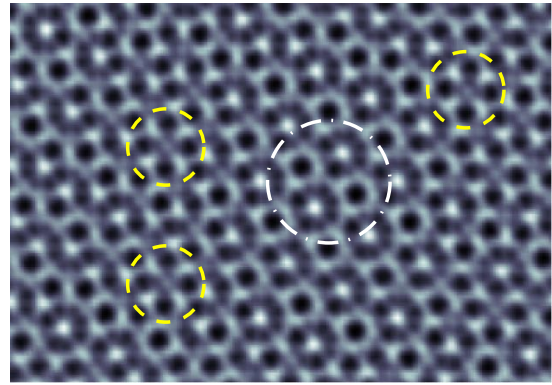


FIG. 4 (color online). Partial view (size  $0.5L \times 0.35L$ ) of 4-mode pattern for  $\rho = 1.2$ . Parameters as in Fig. 2.

peared for early times, they were replaced for  $\rho \geq 1.1$  by domains of patterns comprised of four or more modes, which have lower energy. A condensed view of the temporal evolution of the patterns for different values of the forcing  $\rho$  is given in Fig. 6. It depicts the evolution of the relevant number of Fourier modes  $e^S$ , estimated by the spectral pattern entropy  $S \equiv -\sum_{ij} p_{ij} \ln p_{ij}$ . Here  $p_{ij}$  denotes the normalized power spectrum. Clearly, the number of significant modes increases with  $\rho$ , albeit not monotonically at all times.

In conclusion, we have shown that, in systems undergoing a Hopf bifurcation to spatially homogeneous oscillations, multifrequency forcing can substantially reduce the competition between modes of different orientation leading to complex multimode patterns. By an appropriate choice of the amplitudes and phases of the forcing function, which constitute external control parameters, this regime should be accessible *generically*, essentially independent of the specifics of the unforced system. Our results should therefore apply to realistic chemical oscillators [6,17,24]. From a practical point of view, it should be mentioned, however, that the complex patterns possibly arise only very close to onset. This may require systems

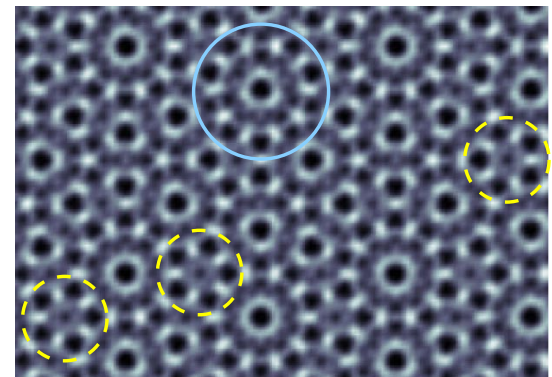


FIG. 5 (color online). Partial view (size  $0.5L \times 0.35L$ ) of 5-mode pattern for  $\rho = 2$ . Parameters as in Fig. 2.

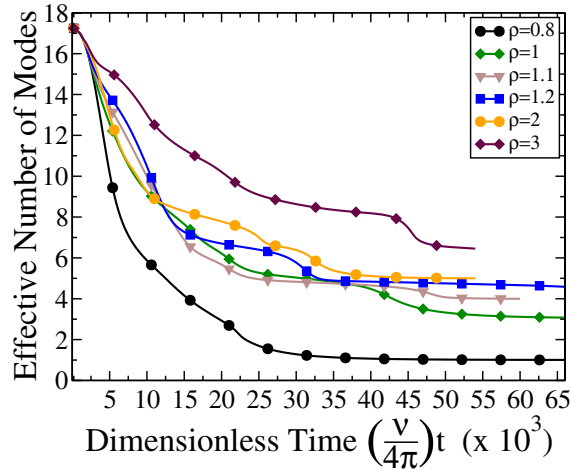


FIG. 6 (color online). Temporal evolution of the relevant number of Fourier modes  $e^S$  for various values of the 1:3-forcing strength  $\rho$ . Parameters as in Fig. 2.

with relatively large aspect ratios and a very precise tuning of the forcing parameters.

By using direct simulations of the complex Ginzburg-Landau equation, we confirmed that these complex patterns arise from general random initial conditions. The appropriate, quantitative characterization of the transients, in which multimode structures such as supersquares and antisquares compete with each other, is still an open problem (cf. [25]). Another interesting question is the long-time scaling of the ordering of such complex structures.

Compared to the Faraday system, the forced Hopf bifurcation considered here allows an additional level of complexity by going slightly *above* the Hopf bifurcation. There, complex patterns may compete with spatially homogeneous oscillations. For single-frequency forcing, labyrinthine stripe patterns arise from the oscillations through front instabilities and stripe nucleation [24]. It is not known what happens to this scenario when the stripes are unstable to the more complex patterns discussed here.

We gratefully acknowledge discussions with A. Rucklidge and M. Silber. This work was supported by NSF Grants No. DMS-322807 and No. DMS-0309657. H. R. thanks the Alexander von Humboldt Foundation for support.

[1] B. Christiansen, P. Alstrom, and M. T. Levinsen, Phys. Rev. Lett. **68**, 2157 (1992); W. S. Edwards and S. Fauve,

Phys. Rev. E **47**, R788 (1993); M.-T. Westra, D. J. Binks, and W. van de Water, J. Fluid Mech. **496**, 1 (2003); Y. Ding and P. Umbanhowar, Phys. Rev. E **73**, 046305 (2006).

- [2] H. Arbell and J. Fineberg, Phys. Rev. Lett. **81**, 4384 (1998); A. Kudrolli, B. Pier, and J. Gollub, Physica (Amsterdam) **123D**, 99 (1998).
- [3] R. Herrero *et al.*, Phys. Rev. Lett. **82**, 4627 (1999).
- [4] J. L. Rogers, M. F. Schatz, O. Brausch, and W. Pesch, Phys. Rev. Lett. **85**, 4281 (2000).
- [5] H.-K. Ko, J. Lee, and K. J. Lee, Phys. Rev. E **65**, 056222 (2002).
- [6] V. Petrov, Q. Ouyang, and H. L. Swinney, Nature (London) **388**, 655 (1997); M. Bertram, C. Beta, H. H. Rotermund, and G. Ertl, J. Phys. Chem. B **107**, 9610 (2003); M. Orban, K. Kurin-Csorgei, A. M. Zhabotinsky, and I. R. Epstein, Faraday Discuss. **120**, 11 (2002).
- [7] I. Berenstein *et al.*, Phys. Rev. Lett. **91**, 058302 (2003).
- [8] N. D. Mermin and S. M. Troian, Phys. Rev. Lett. **54**, 1524 (1985).
- [9] A. C. Newell and Y. Pomeau, J. Phys. A **26**, L429 (1993).
- [10] B. Malomed, A. A. Nepomnyashchy, and M. I. Tribelsky, Sov. Phys. JETP **69**, 388 (1989).
- [11] M. Silber, C. M. Topaz, and A. C. Skeldon, Physica (Amsterdam) **143D**, 205 (2000).
- [12] J. Porter, C. M. Topaz, and M. Silber, Phys. Rev. Lett. **93**, 034502 (2004).
- [13] W. Zhang and J. Vinals, Phys. Rev. E **53**, R4283 (1996).
- [14] A. M. Rucklidge and M. Silber, Phys. Rev. E **75**, 055203(R) (2007).
- [15] P. Coulet, T. Frisch, and G. Sonnino, Phys. Rev. E **49**, 2087 (1994).
- [16] J. M. Conway and H. Riecke, Phys. Rev. E **76**, 057202 (2007).
- [17] A. L. Lin, A. Hagberg, E. Meron, and H. L. Swinney, Phys. Rev. E **69**, 066217 (2004).
- [18] The form of (1) is determined by the behavior of  $\gamma$  and  $\rho$  under shifts of the fast time  $\hat{t} \rightarrow \hat{t} + \Delta\hat{t}$ :  $\gamma \rightarrow \gamma e^{2i\omega_h \Delta\hat{t}}$  and  $\rho \rightarrow \rho e^{3i\omega_h \Delta\hat{t}}$ . [cf. P. Coulet and K. Emilsson, Physica (Amsterdam) **61D**, 119 (1992).]
- [19] J. M. Conway and H. Riecke (to be published).
- [20] B. Dionne, M. Silber, and A. C. Skeldon, Nonlinearity **10**, 321 (1997).
- [21] M. Higuera, H. Riecke, and M. Silber, SIAM J. Appl. Dyn. Syst. **3**, 463 (2004).
- [22] B. Echebarria and H. Riecke, Physica (Amsterdam) **158D**, 45 (2001).
- [23] A. M. Rucklidge and W. J. Rucklidge, Physica (Amsterdam) **178D**, 62 (2003).
- [24] A. Yochelis *et al.*, SIAM J. Appl. Dyn. Syst. **1**, 236 (2002).
- [25] H. Riecke and S. Madruga, Chaos **16**, 013125 (2006).